Research Article
doi.org/10.1002/elsa.202300018

Chemistry Europe
European Chemical Societies Publishing

Received: 10 June 2023
Revised: 24 July 2023
Accepted: 25 July 2023

Optical, vibrational, electrical, and electrochemical studies of new plasticized methylcellulose-based solid polymer electrolytes for supercapacitor application

Theodore Manfo Azemtsop

Department of Electrical and Electronics Engineering, Faculty of Engineering and Architecture, Recep Tayyip Erdogan University, Center/RIZE, Turkey

Correspondence
Theodore Manfo Azemtsop, Recep Tayyip Erdogan University, Faculty of Engineering and Architecture, Zihni Derin Campus – Fener Str., 53100, Center/RIZE, Turkey.
Email: azemsouleymane@yahoo.fr

Abstract

In this work, new plasticized solid polymer electrolytes (SPEs) are developed using MC (methylcellulose) as a polymer host, and sodium iodide (NaI) as a dopant via the solution casting method. Ethyl carbonate (EC) is used as a plasticizing agent to improve the properties of the SPEs. Polarized optical microscopy analysis reveals that the surface morphology of the MC-NaI-EC films contained porous amorphous regions owing to the presence of EC. The complex formation between MC, NaI, and EC is confirmed by Fourier-transform infrared spectra. The addition of EC in the MC-NaI polymer salt matrix enhances the electrochemical properties of the prepared films. The highest ionic conductivity of 5.06×10^{-3} S/cm is achieved for the composition: MC+50 wt. % NaI +10 wt. % EC. The linear sweep voltammetry test reveals that the optimal plasticized-SPE can withstand up to 2.5 V. The ionic transference number analysis reveals that 99% of ions contribute to the total conductivity. The optimized SPE film and graphene oxide-based electrodes are used to manufacture a solid-state electrical double-layer capacitor. The coulomb efficiency of the supercapacitor cell is 100%, and the specific capacitance of the supercapacitor is found to be 18.56 F/g utilizing impedance data at low frequency.

KEYWORDS
EDLC, Ionic conductivity, methylcellulose, polymer electrolyte, transference number

1 | INTRODUCTION

In recent years, there has been a lot of interest in flexible and portable energy storage devices, bendable displays, artificial skins, and portable electronic gadgets.[1–3] Energy is stored in an electrical double-layer capacitor (EDLC) device as a result of the build-up of charges at the interface between the electrolyte and the electrode.[2]

Solid polymer electrolyte (SPE) is an emerging candidate for manufacturing future energy storage systems at a low price and reducing the leakage and corrosion at the electrode.[4] PEs with excellent chemical, thermal and mechanical properties as well as their good water absorption, are required for good conductivity.[5] Green biopolymers deteriorate generally, whereas human fabricated polymers are remarkably non-biodegradable[6]

Research Article
doi.org/10.1002/elsa.202300018
Chemistry Europe
European Chemical Societies Publishing

Cellulose is one of the most abundant green polymers present in nature; however, pure cellulose is not soluble in water,[7] and thus, needs to be modified. The use of methyl chloride in cellulose named methylation appears as a solution to dissolve cellulose. The methylation will form methyl cellulose (MC) which can dissolve in water. MC contains lone pair electrons at its oxygen atoms, which can act as complexation sites with the salt's cation. The existence of lone pair electrons is a need for a polymer to host ionic conduction.[8] Cations in sodium iodide (NaI) can coordinate with O_2 atoms present in MC over dative bonds. As a benefit in terms of conductivity, the functional groups present in MC such as C– O–C, O–H, and O–CH_3 have segregated pair electrons that are in charge of ion transport.[9] In addition, MC polymer has an amorphous structure, exhibiting a quite high glass transition temperature (T_g), in the range of 184–200°C.[10]

Supercapacitors' long life cycles and high power density make them ideal energy storage devices.[11] Charges accumulate and are released at the electrolyte/electrode contacts in EDLCs. Many EDLCs are manufactured using various electrode materials such as graphite, activated carbon (AC), carbon nanogel, and carbon nanotubes (CNTs). However, the EDLC device appears to be a potential alternative to traditional batteries, particularly in low energy density applications. As EDLC stores energy through the process of adsorption or desorption, or a non-Faradaic process, a large surface area electrode is crucial.[12] The performance of EDLC might be increased by modifying the electrolytes or electrodes. Conventional accomplishments have demonstrated that PEs are appropriate because of their solvent-free, leakage-free, easy formation of thin films, easy manageable, and extensive electrochemical windows as opposed to commercial liquid electrolyte counterparts.[13,14] Ammonium salts integrated into MC have been the subject of much research to generate PEs,[15,16] nonetheless, there has been minimal focus on PEs, especially sodium salts. Sodium is plentiful and less expensive than lithium. Furthermore, because the materials are soft, it is simpler to create and maintain contact with other battery components.[17] Aziz et al.[11] prepared compatible green polymer electrolytes based on methylcellulose (MC) and NaI for EDLC application. The solution casting technique was used to make green SPE using different amounts of NaI. The maximum conductivity of the optimized MC-NaI sample was determined to be 3.01×10^{-3} S/cm with 50 wt. % NaI. The incorporation of NaI into MC has increased the ion transfer number from 0.75 to 0.93. The electrochemical stability potential window was about 1.7 V. The EDLC delivers a high capacitance of 94.7 F/g. Abdullah et al.[18] prepared SPEs using polyvinyl alcohol (PVA)/MC incorporated with NaI salt. The highest value of ionic conductivity was determined to be 1.53×10^{-5} S/cm for the composition 50 wt. % NaI. The X-ray diffraction (XRD) result reveals the optimal sample provides the lowest degree of crystallinity. Ismayil et al.[19] prepared SPE films using the solution casting method. The effect of NaI on a polymer blend matrix composed of sodium carboxymethyl cellulose (NaCMC) and PVA was investigated. The results show that the highest conductivity of NaCMC/PVA-based SPE film was about 2.52×10^{-3} S/cm for 30 wt. % NaI. The incorporation of NaI into the NaCMC/PVA matrix has decreased the crystallinity of SPE film as revealed by the XRD data. Fourier-transform infrared (FTIR) approach confirmed the complexation between NaI, NaCMC, and PVA due to the formation of Na^+ and –OH groups and hydrogen bonds between the I^- and –CH groups. The salt incorporation has promoted the number of ions but still shows a thermal stability decrease. Transference number measurement (TNM) measurements showed that the ion transference number of the optimized film was 0.99.

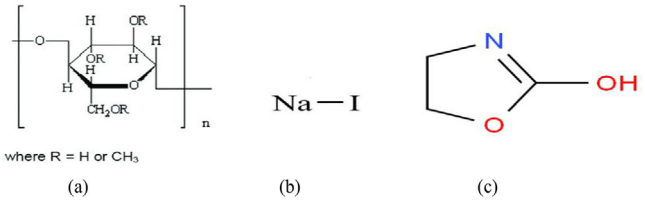

FIGURE 1 Chemical structure of (a) pristine methylcellulose (MC), (b) sodium iodide (NaI), and (c) ethyl carbonate (EC).

This work uses MC as a host polymer to prepare an essential, eco-friendly, sustainable PE. The addition of NaI as additive material and ethyl carbonate (EC) as a plasticizer to the polymer matrix helps to improve ionic conductivity. The structural morphology, physical, and electrochemical properties of the plasticized SPEs will be investigated as well as the performance of the solid-state EDLC based on the optimized plasticized SPE film.

2 | MATERIALS AND METHODS

MC (Mw: 658.7 g/mol), NaI (Mw: 40,000 g/mol), and EC (Mw: 88.06 g/mol) are used as purchased to prepare the SPE films. The chemical structure of each material is shown in Figure 1. MC was used as the host polymer, NaI as an ion supplier, EC as a plasticizer, and double-distilled water (DDW) as solvent. All the materials were bought from Sigma-Aldrich. Each SPE film was characterized using the Motic (BA 310 model) to perform the POM, a Perkin-Elmer FTIR spectrometer (model RX1) was used to conduct the FTIR measurements, and the electrochemical impedance spectroscopy (EIS) measurement was made by way of CH instruments CHI660D (Model 600 series electrochemical analyzer/workstation).

Research Article
doi.org/10.1002/elsa.202300018
Chemistry Europe
European Chemical Societies Publishing

TABLE 1 The composition of the ethyl carbonate (EC)-based quasi-solid polymer electrolyte (quasi-SPE) films.

Samples	MC(g)	NaI (wt. %)	EC (wt. %) EC (g)
MCSPE0	1	50	0 0
MCSPE1	1	50	10 0.111
MCSPE2	1	50	20 0.250
MCSPE3	1	50	30 0.428
MCSPE4	1	50	40 0.666

2.1 | Polymer salt synthesis without plasticizer

A chosen amount of 1 g of MC powder was dissolved in 80 ml DDW and stirred for a few hours till a completely dissolved solution is obtained at room temperature (RT). Afterward, a fixed quantity of 50 wt. % NaI was then introduced to the MC solution and mixed again for several hours. Four identical solutions of MC: NaI polymer salt were prepared.

2.2 | Polymer salt synthesis with plasticizer

The four solutions were subsequently doped with EC at various concentrations (0, 10, 20, 30, and 40 wt. %) and swirled continuously for the whole day until transparent homogeneous solutions are obtained. The samples were named MCSPE0, MCSPE1, MCSPE2, MCSPE3, and MCSPE4 which matched 0, 10, 20, 30, and 40 wt. % EC, respectively. Each solution was then put into a petri dish and let dry for a week in a desiccator filled with silica gel powder. Plasticized-SPEs were obtained with different EC contents. Table 1 lists the components of the MC-based SPE samples as well as their contents.

2.3 | Measurements

All the prepared films of pure MC, MC- NaI, and MC-NaI: EC-based PEs with different EC concentrations were characterized. The electrochemical work-station CH-instrument (USA model) was used to perform the EIS, linear sweep voltammetry (LSV), TNM, and cyclic voltammetry (CV) analyses across a frequency range of 0.01–1 MHz.

2.3.1 | POM approach

Motic Optical Microscopy (BA 310 model) was used to investigate the surface morphology of the samples to assess the influence of the EC on the MC-NaI polymer salt complex.

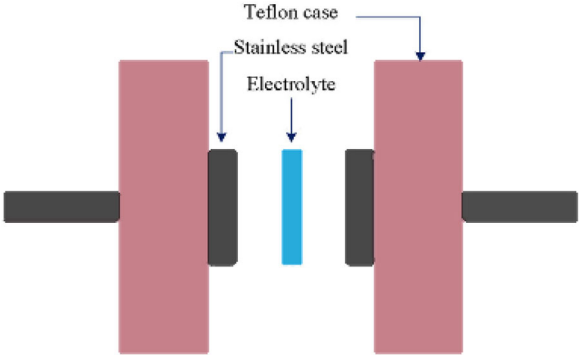

FIGURE 2 The schematic diagram for TNM, linear sweep voltammetry (LSV), and impedance investigations.[16]

2.3.2 | FTIR approach

The distinct polymer-ion interactions and particular functional groups present in MC-based plasticized SPE samples are measured using a Perkin-Elmer FTIR spectrometer (RX1) at 25°C spanning the range 4000–650 cm^{-1} at a resolution of 4 cm^{-1}. This method was also used to verify the complexity of MC, NaI, and EC.

2.3.3 | EIS approach

The electrical behavior of the MC-NaI: EC-based SPE film was examined via the EIS method, which relies on the frequency of AC potentials. This approach also measures the impedance between the SPE and the electrode. This resistance value varies with the concentration of EC added to the MC-NaI polymer salt.

Ionic conductivity

Ionic conductivity (σ) was determined by embedding each PE film between two stainless steel electrodes, as illustrated in Figure 2. The ionic conductivity was determined using the conventional formula.[16]

$$\sigma = \frac{d}{R_b \times A} \quad (1)$$

where R_b is the bulk resistance, A is the film's section area ($1 \times 1 cm^2$) of the film, and d is the sample thickness determined using a screw gauge (0–25 mm).

Relative permittivity

Relative permittivity ($\mathcal{E}$) was measured for each sample using Equation (2):

Research Article
doi.org/10.1002/elsa.202300018

$$\mathcal{E}^* = \mathcal{E}' - j\mathcal{E}'' = \frac{1}{j\omega\mathcal{E}_0 Z^*} \quad (2)$$

The complex impedance data at 1 kHz frequency is used to determine the relative permittivity values. The real($\mathcal{E}'$) and imaginary and ($\mathcal{E}''$)components of the complex permittivity ($\mathcal{E}^*$) are calculated using Equations (3) and (4), respectively:

$$\mathcal{E}' = \frac{Z''}{(Z''^2 + Z'^2)\omega C_0} \quad (3)$$

$$\mathcal{E}'' = \frac{Z'}{(Z''^2 + Z'^2)\omega C_0} \quad (4)$$

where $Z'$and $Z''$are real and imaginary parts of impedance spectroscopy (Z^*), ω is the angular frequency ($\omega = 2\pi f$), $C_0 = \mathcal{E}_0 \frac{A}{d}$ is the free space capacitance and $\mathcal{E}_0$, vacuum permittivity.

Carrier density and mobility

Carrier density (n_0) and mobility(μ) may be calculated using Equations (5) and (6) respectively[20]:

$$n_0 = \left[\frac{\sigma_0}{3\mathcal{E}_0\mathcal{E}'_s\,\omega_{10\mathcal{E}}}\right]^4 \frac{\mathcal{E}_0\mathcal{E}'_s KT}{e^2 d^2} \quad (5)$$

where σ_0 denotes quasi-dc conductivity, e elementary charge, K and T denote the constant of Boltzmann and the thermodynamic temperature, respectively, and the efficient relative permittivity is written as[21] $\mathcal{E}'(\omega_{10\mathcal{E}}) = 10\mathcal{E}'_s$. Where $\mathcal{E}'_s$ is the real part of the effective permittivity.

The carrier mobility is then estimated using the relationship shown below[20,21]:

$$\mu = \frac{\sigma_0}{en_0} \quad (6)$$

2.3.4 | LSV method

This tool is used to check the maximum potential voltage of the optimized SPE film. The LSV method can also measure the current between the reference and working electrodes.

2.3.5 | Ionic transference number

Wagner's polarization approach is used to determine the contribution of ions and electrons in the plasticized SPE film. The film is scanned between two stainless steel plates at a constant scan rate, and the current density is recorded over time. The total conductivity can be evaluated through the calculation of the ion transference number (t_{ion}) and electron transference number (t_{elec}) using Equations (7) and (8) shown below[22]:

$$t_{ion} = \frac{I_i - I_{ss}}{I_i} \quad (7)$$

$$t_{elec} = 1 - t_{ion} \quad (8)$$

where I_{ss} and I_i are the steady-state and total currents, respectively.

2.4 | Material synthesis of electrodes

The exfoliation approach was used to prepare graphene oxide (GO) as electrode material.[23] A solution of GO was formed by the mixture of DDW and H_2SO_4 in the proportion 10: 90 wt% respectively. Electric wires connected to both platinum cable and graphite are first bonded to a power supply before being inserted in the prepared solution. The entire system was covered with a paraffin membrane, and a fixed voltage of 4 V was supplied for 5 h to finish the exfoliation process. The resultant dark solution was completely ultrasonicated, cleansed, purified, desiccated, and collected. The finished product was then baked at 80°C.

2.5 | Fabrication and testing of a solid-state EDLC

2.5.1 | EDLC manufacturing

Electrode production

The optimized MC-NaI-EC-based SPE film and two identical electrodes were utilized to create the supercapacitor device. Clean 1 × 1cm^2 graphite sheets were used to make the electrodes, which were then doped with an active substance. The process for creating the active substance involved dissolving P (VDF-HFP) as a binder in a very little amount of acetone (solvent), combining it with GO in a 10:90 wt. %, and crushing it to create a homogenous slurry. The graphite sheets were then evenly covered with the GO paste and dried overnight in an oven at 80°C.

Finally, the high ion-conducting plasticized SPE sample was sandwiched between two GO-based electrodes to make an EDLC cell. The various parts of the completed EDLC are shown in Figure 3.

2.5.2 | An analysis of the EDLC cell

Cyclic voltammetry

CV is used to examine the nature of charge storage at the electrolyte-electrode interface as well as its performance across a set voltage range. The CV approach can be used

Research Article
doi.org/10.1002/elsa.202300018

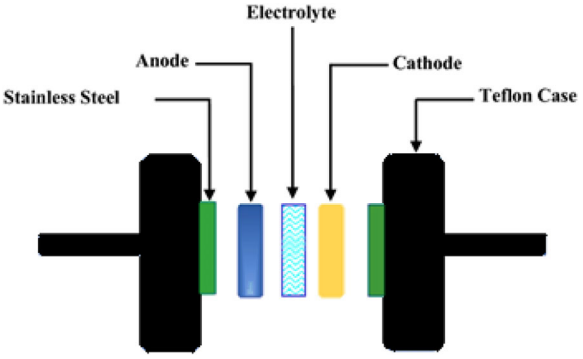

FIGURE 3 The schematic diagram for the cyclic Voltammetry (CV) and supercapacitor measurements.[23]

to analyze the nature of the charges stored in the EDLC cells at the interfacial area in the anodic and cathodic regions.[24] The EDLC was assembled and tested using the CV approach at a fixed scan rate. The area of the capacitive buckling of the CV graph was determined using an integration function in Origin 8.5 software, and the specific capacitance of the EDLC was derived using Equation 9:

$$C_{sp} = \int_{V_1}^{V_2} \frac{I(V)\,dV}{2mS(V_2 - V_1)} \tag{9}$$

where m denotes the mass of active material (GO), V is the voltage, and S is the scan rate.

Galvanostatic charge-discharge

The galvanostatic charge-discharge (GCD) approach is experimentally opposed to the CV method where the variations of charges and discharges are observed within a voltage range under a fixed applied current. This tool displays the real performance of the cell. The coulombic efficiency was determined using Equation (10):

$$\eta = \frac{\Delta t_D}{\Delta t_C} \times 100\% \tag{10}$$

where Δt_D represents the discharging time and Δt_C represents the charging time. The specific capacitance (C_{sp}) of the supercapacitor was obtained by exploiting the GCD data using Equation (11):

$$C_{sp} = \frac{I}{(dV/dt)\,m} \tag{11}$$

where I, is the discharge current, dV/dt is the slope of the discharge curve, and m is the mass of the GO.

EIS approach

This tool was employed to evaluate C_{sp}. The value of C_{sp} is obtained using the following expression:

$$C_{sp} = \frac{-1}{2\pi f Z'' m} \tag{12}$$

where $Z''$is the imaginary part of impedance at lower frequencies, m is the active electrode material (GO) and f is the frequency.

3 | RESULTS

3.1 | POM analysis

To comprehend the compatibility between each component of the plasticized SPEs, the study of the phase transitions can be monitored using the POM approach. Figure 4 presents the micrographs of pure MC, NaI, EC, MC-NaI, and the optimized MC-NaI: EC-based SPE film. The surface morphology of each sample film looks uniformly homogeneous with no phase separation. Figure 4a shows the surface morphology of Pristine MC. The morphology of MC appears compact and an obvious interconnected porous structure is observed. The morphology of the MC sample also reveals traces of scratches and damages, which characterize the substrate-surface state. The scratches and damages appear due to the roughness of the surface of the petri dish used to prepare the MC film. The structure of the pure MC film is seen to be poorly organized. The surface morphology of MC exhibits spherulite and microspores with different sizes dispersed along the surface of the pure film. Previous research has proven that spherulite is associated with the crystalline area, while the dark regions between spherulite contacts are associated with the amorphous phase.[25] The presence of the spherulites with small amorphous regions between the spherulites in the morphology confirms that MC is semi-crystalline. Figure 4b,c shows the surface morphology of NaI and EC respectively. The inclusion of 50 wt. % NaI in the MC matrix has crucially changed the morphology of MC: NaI PE as shown in Figure 4d. It is observed a reduction in the size of the MC spherulites and consequently an increase of darker regions upon the addition of NaI salt, implying a reduction in crystallinity. The MC: NaI sample morphology is uniform and homogeneous, although with various levels of roughness due to the addition of NaI salt. It has been shown that salt ions can combine with polymer chains to create complexes, which diminish hydrogen bonding interactions within the polymer matrix and increase the percentage of amorphous material.[26] Previous research has postulated that rough surfaces connecting PEs act as conduits for ion conduction via the electrolyte.[27–29] Additionally, the production of ion pairs, which is unrelated to the ionic conduction process, was described as the emergence of particles on the surface of samples.[30–32] At high

Research Article
doi.org/10.1002/elsa.202300018
Chemistry Europe
European Chemical Societies Publishing

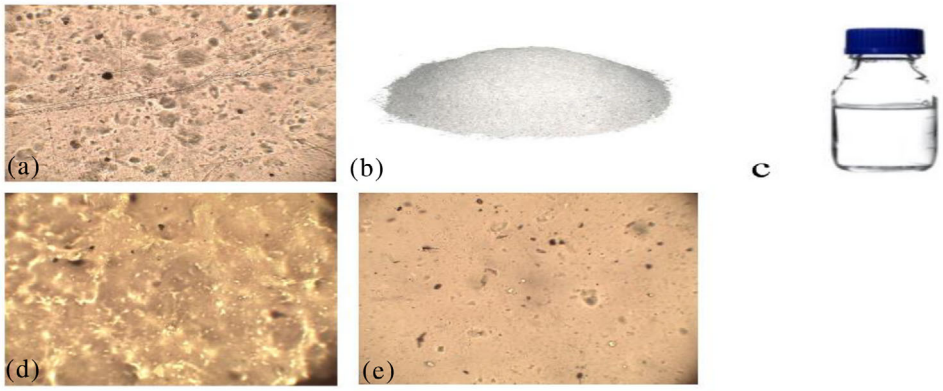

FIGURE 4 Micrographs of (a) Pristine methylcellulose (MC) film, (b) sodium iodide (NaI), (c) ethyl carbonate (EC), (d) MC+50 wt% NaI, and (e) MC + 50 wt% NaI + 10 wt% EC film taken at (10) magnifications with and a scale bar of 100 μm.

salt concentrations, salt can aggregate due to the inter-ionic electrostatic interactions and the incompatibility of the integrated salt with the polymer. Ion pairs are created when the salt concentration exceeds a certain level, which causes salt to flow to the surface. It is clear from the POM micrograph image that the sample's surface contains tiny white specks. Bhad and Sangawar, who combined PVA with NH_4SCN salt, also noted this effect.[33] They observed that the white flecks on the outer layer of the electrolyte can behave as proton conductors. The incorporation of 10 wt. % EC into the polymer-salt matrix has significantly reduced the number of white particles (aggregates) in the morphology of the sample with increased dark regions (Figure 4e). The dark regions appear due to the plasticizing effect of EC which increases the amorphousness of the EC-based SPE film. The reduction in salt aggregation (ion clusters) suggests ion dissociation into the matrix. The ionic dopant NaI is thought to dissociate more quickly in the presence of EC, increasing the dissociation of Na^+ toward the MC matrix. EC provides a structure with a shortened path, allowing Na^+ to go through and pass each point more quickly. During the transfer phase, weak bonds formed between Na^+ and the oxygen atoms of the EC earlier than the Na^+ leaped to the C = O of the SPE. The energy threshold was also lowered as a result of the decreased effective hop distance.[34] As a result, the incorporation of EC into the MC: NaI matrix has significantly modified the surface by reducing the formation of white agglomerates due to the non-complete dissociation of salt. It can be observed that the plasticized SPE had a smooth surface with no apparent defects. The surface morphology also changed from bright to dark with an increase in some dark regions that confirms the increase in amorphous nature caused by the plasticizing effect of EC. EC as a plasticizer has not only increased the amorphousness of the plasticized SPE but also facilitated the dissolution of some ion-aggregates present in MC: NaI,

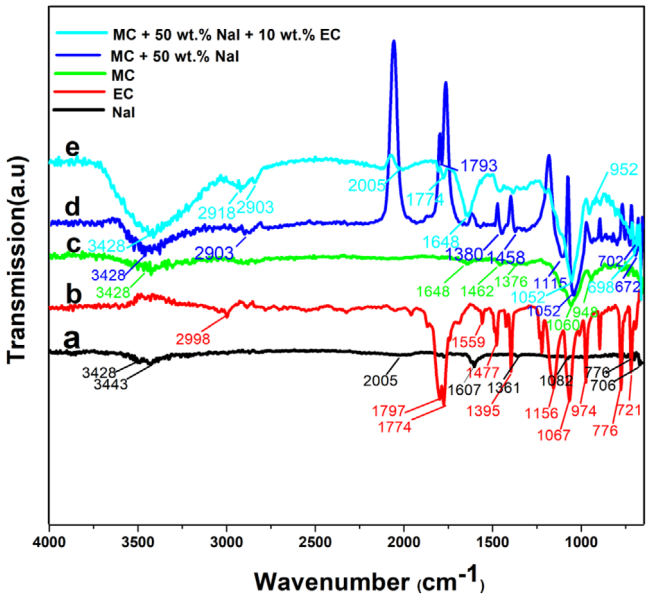

FIGURE 5 Infrared (IR) spectra of (a) sodium iodide (NaI), (b) ethyl carbonate (EC), (c) Pure methylcellulose (MC), (d) MC + 50 wt.% NaI and (e) MC+50 wt.% 10 wt.% ethyl carbonate (EC) recorded at room temperature (RT) with a spectral resolution of 4 cm^{-1}.

which increases the number of free ions and thus enhances the ionic conductivity.

3.2 | FTIR spectroscopy

The complex formation between the polymer, salt, and plasticizer was investigated using FTIR spectroscopy. The IR spectra of NaI, EC, pure MC, polymer-salt, and the optimal plasticized SPE film are shown in Figure 5. The IR spectrum of pure NaI is shown in Figure 5a. Some absorption peaks are visible at 3428, 3443, 2005, 1987, 1607,

Research Article
doi.org/10.1002/elsa.202300018
Chemistry Europe
European Chemical Societies Publishing

1361, 1082, 776, and 706 cm^{-1}. Figure 5b depicts the IR spectrum of pure EC. There are obvious vibration peaks that can be seen clearly at 2996, 1797, 1774, 1559, 1477, 1395, 1156, 1067, 974,776, and 721 cm^{-1}. Figure 5c reveals the IR spectrum of pure MC. A stretching vibration of O–H at 3428 cm^{-1} and C = C stretch at 1462 cm^{-1} suggested the presence of alcohols and aromatic compounds. A strong peak of C–O was observed at 1060 cm^{-1} and the bending vibration of = C–H at 948 cm^{-1} suggested the presence of alcohol and alkenes respectively. Additionally, two minor vibrational bands were seen at 1648 and 1376 cm^{-1}. Figure 5d shows the IR spectrum of the MC: NaI which features the interaction between MC and NaI. The presence of a broad and strong peak at 3428 cm^{-1} assigned to the O-H stretch and the vibration of the C–H stretch at 2903 cm^{-1} revealed the existence of alcohols and alkanes, respectively. A strong band of stretching vibration of C = O at 1793 cm^{-1} and a medium band of = C–H observed at 1458 cm^{-1} were assigned to acid chlorides and aromatics respectively. Two strong absorption peaks of C–O at 1380 and 1052 cm^{-1} were ascribed to alcohols. Finally, the two absorption peaks observed at 702, and 672 cm^{-1} corresponding to the C–H bend vibration were assigned to aromatic compounds. Figure 5e depicts the IR spectrum of the EC-based MC: NaI, which indicates the existence of vibration bands. A vibratory stretching of O–H at 3428 cm^{-1} suggested the presence of alcohol groups. Two absorption peaks were found at 2918 and 2903 cm^{-1} both of which correlate to C–H stretching and are ascribed to alkanes and alkyl groups. A strong band of C = O stretches at 1648 cm-^{1} and a strong band of C-H bending at 698 cm^{-1} is attributed to amide and aromatic compounds, respectively. The bending vibration of = C–H was detected at 695 cm^{-1}, indicating the presence of alkenes. Finally, four vibrational bands were found in the EC-doped MC: NaI spectrum at 2005, 1774, 1052, and 952 cm^{-1}. The changes in peak intensities and positions observed in IR spectra of the MC: NaI complex and the optimal plasticized SPE were caused by phase and chemical composition changes. Some peaks initially present in the pure NaI salt are also found in MC: NaI with a shift in position and intensity. The additional peaks present in MC: NaI at 2903, 1793, 1458, 1380, 1052, 702, and 672 cm^{-1} confirmed the interaction between MC and NaI. Because of the connection of Na^{+} ions to C–O and = C–H stretching both of MC pure MC, the C–O stretching at 1060 cm^{-1} and = C–H at 948 cm^{-1}, have changed to 1052 and 952 cm^{-1} respectively for EC- based MC: NaI sample. It was found that some peaks (3428, 2903, and 1052 cm^{-1}) present in EC-based MC: NaI also appeared in MC: NaI. The existence of additional peaks in EC-based SPE indicated the interaction between NaI, EC, and MC, confirming the formation of a complex.

TABLE 2 Calculated values of RT- σ for the prepared solid polymer electrolytes (SPEs) with their uncertainties.

Samples	σ (S/cm)	σ Error (±)
MC	3.1×10^{-11}	–
MCSPE0	3.02×10^{-3}	1.51×10^{-4}
MCSPE1	5.06×10^{-3}	2.53×10^{-4}
MCSPE2	1.00×10^{-3}	5×10^{-5}
MCSPE3	2.45×10^{-3}	1.225×10^{-4}
MCSPE4	9.09×10^{-4}	4.545×10^{-5}

The highest value of σ was found with the sample MCSPE1: MC + 50 wt. % NaI + 10 wt. % EC and determined to be 5.06×10^{-3} S/cm. The variation in σ with EC content in the MC: NaI matrix is shown in Figure 7.

3.3 | Analysis of AC impedance

The electrical behavior of the plasticized SPE films was carried out using the impedance spectroscopy approach. Figure 6 depicts the Nyquist plots of pure MC, MC-NaI, and plasticized SPE films at RT with EC concentrations of 10, 20, 30, and 40%. The high-frequency region shows a semicircle, whereas the low-frequency area shows a spike. The semicircle is created by the volume effect of the electrolyte, while the spike is caused by the blocking action of the electrodes.[35] The intercept between the semicircle and the spike was used to compute the bulk electrolyte resistance of each sample. The addition of 50% NaI to MC dramatically reduced the diameter of the semi-circle, implying a reduction of bulk resistance in NaI- doped MC. The rise in the carrier density induced by the inclusion of NaI might account for this decrease. The incorporation of different concentrations of EC into the MC: NaI matrix has also contributed to lowering bulk resistance, which may be related to increased polymer chain mobility. This decrease in semicircle diameter suggests an increase in ionic conductivity. It should be noticed that pure MC shows a conductivity of 3.1×10^{-11} S/cm, as computed from Figure 6a. The conductivity increases to 3.02×10^{-3} S/cm when the salt is dispersed in pure MC (Figure 6b). Impedance spectroscopy of the EC-based plasticized SPEs is observed in Figure 6c–f. The highest conductivity value is found to be 5.06×10^{-3} S/cm for the sample: MC + 50 wt% NaI + 10 wt% EC (MCSPE1) with the lowest value of bulk resistance.

3.3.1 | Conductivity measurements

The ionic conductivity (σ) of each sample was determined using Equation (1). Table 2 summarizes the values of σ for various concentrations of EC calculated at RT.

The addition of the optimal amount of 50 wt. % NaI in MC leads to enhance σ in pure MC from 3.1×10^{-11} to 3.02×10^{-3} S/cm. The incorporation of EC as a plasticizing

Research Article
doi.org/10.1002/elsa.202300018
Chemistry Europe
European Chemical Societies Publishing

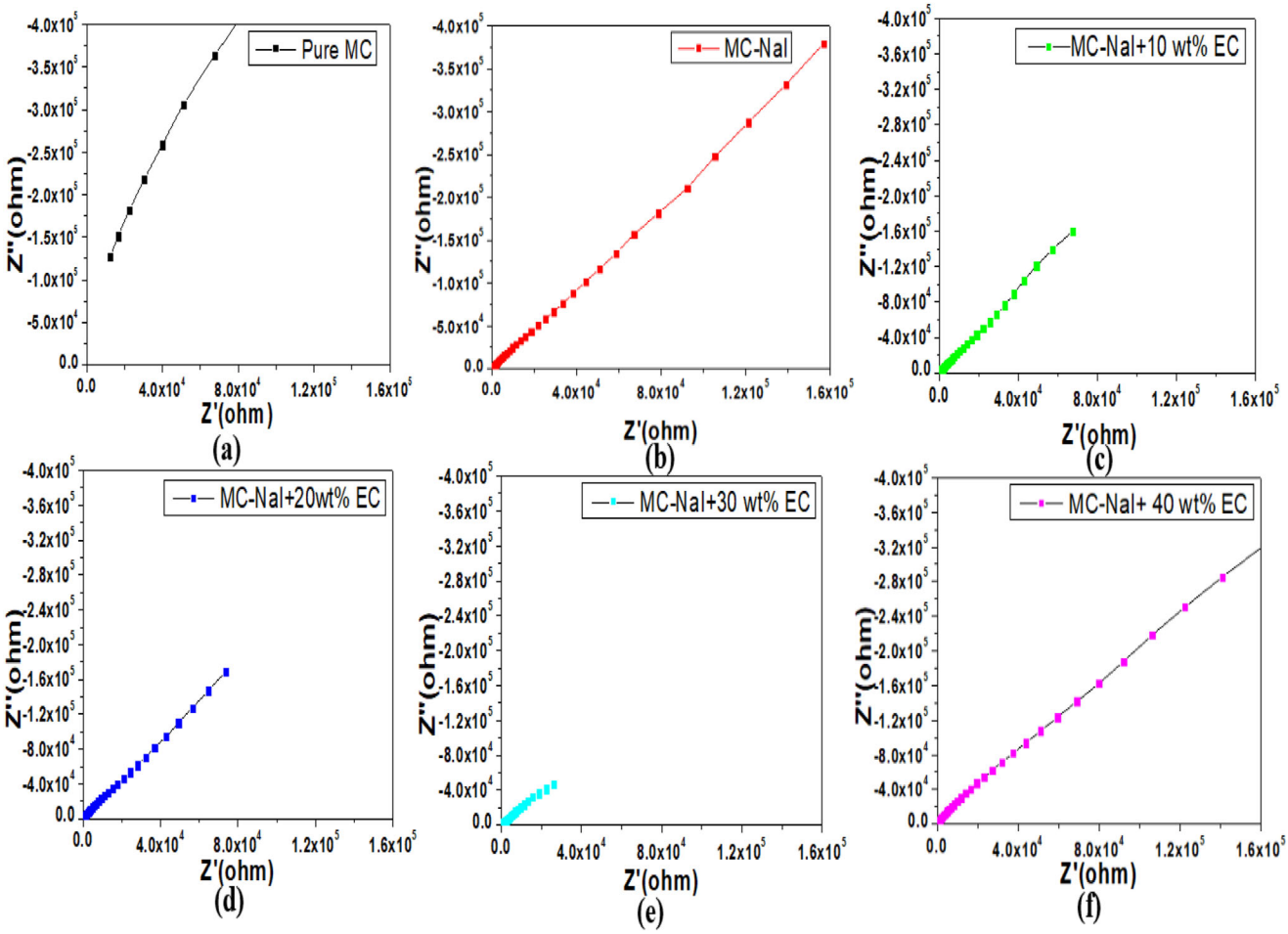

FIGURE 6 Nyquist plot for plasticized SPE samples: (a) Pure methylcellulose (MC), (b) MCSPE0, (c) MCSPE1, (d) MCSPE2, (e) MCSPE3, and (f) MCSPE4 at room temperature (RT).

agent into the MC: NaI matrix has also contributed to conductivity. The σ reaches a maximum value of 5.06×10^{-3} S/cm upon inclusion of 10 wt. % EC. Figure 7 shows the conductivity trend in MC: NaI with various EC concentrations. The initial rise in σ was observed upon the addition of 10 wt. % EC. This augmentation was related to the rise in mobility caused by the plasticizing impact of EC in the MC: NaI matrix which decrease the glass transition temperature. The increased flexibility of the polymer chain contributed to reducing the crystallinity and thus increases the conductivity. The ion-association theory may be responsible for the further decrease in σ at a greater amount of EC, which leads to generating ion clusters and a fall in carrier concentration. With the direct coordination of the solvent molecules and CO_3^{2-}anions from EC, complicated ion-pair complexes were formed. Na^+ ions were entirely solvated by solvent molecules after a direct interaction between solvents molecules and CO_3^{2-}anions leading to generate ion pair complexes. The further rise in conductivity up to 2.45×10^{-3} S cm^{-1} at a high concentration of 30 wt. % EC was because of the segregation

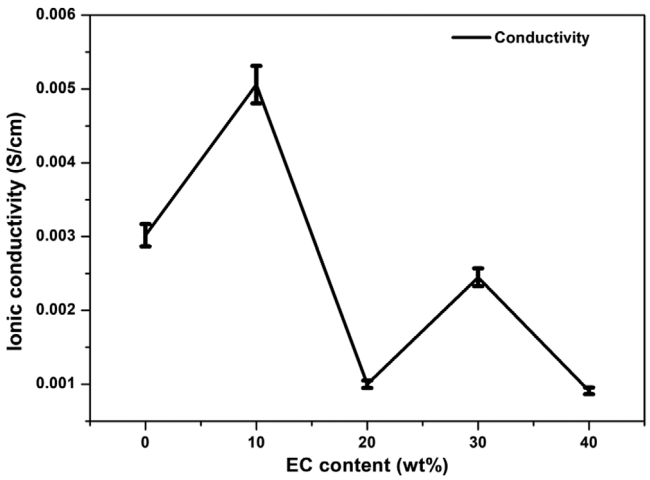

FIGURE 7 Ionic conductivity versus ethyl carbonate (EC) content in plasticized solid polymer electrolyte (SPE): MC + 50 wt. % NaI.

of clusters caused by the relatively high relative permittivity throughout the material especially that of the EC, which became dominant as the EC amount rose. This

Research Article
doi.org/10.1002/elsa.202300018
Chemistry Europe
European Chemical Societies Publishing

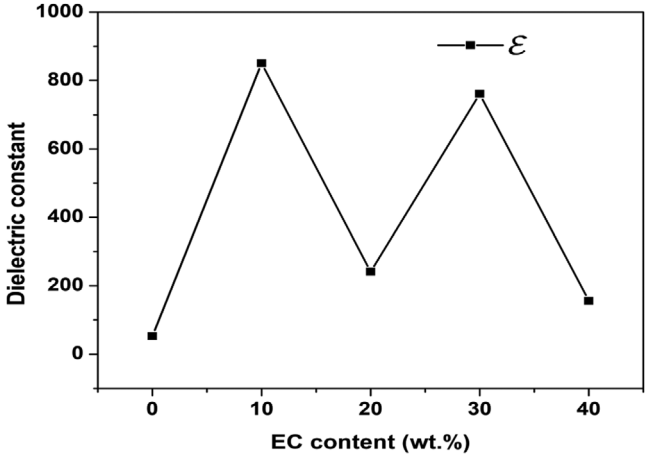

FIGURE 8 Dependence of $\mathcal{E}$ with ethyl carbonate (EC) concentration in MC + 50 wt. % NaI system at 10^3 Hz.

re-dissociation of ion clusters enhanced the carrier density resulting in improving SPE conductivity. However, the density of mobile carriers has a significant impact on $\boldsymbol{\sigma}$.[36–38] The formation of ion-pair complexes as a result of direct interaction between EC, NaI, and MC resulted in the multiplication of mobile charges within the matrix. This salvation resulted in a wide distribution of Na^+, CO_3^{2-} and I^-, leading to a rise in $\boldsymbol{\sigma}$ at 30 wt. % IL. Over 30 wt. %, the inclusion of EC caused a reduction in the, which may have resulted in ion aggregates (clusters). Cluster formation slowed mobility and lowered free ion concentration, resulting in a reduction in conductivity.[39–44] At lower concentrations, EC works as a plasticizer by improving the mobility of the polymeric chain, which increases conductivity; however, a high concentration of EC in the SPE induced the formation of more non-conducting ions which do not contribute to the conductivity. The influence of chain mobility on ionic conductivity could be connected to the polymer's free volume in general. As the free volume within the polymer grows, the polymer chain rotates more easily, and ion transport in PEs accelerates. As a result, the addition of EC increases the free volume of PEs, resulting in increased ionic conductivity. The plasticizer promotes ionic mobility by reducing the viscosity of the ionic environment, resulting in high conductivity at ambient temperature. In the plasticized electrolyte, the Na^+ ions get coordinated with both the polymer and the EC. There are additional interactions between the polymer chain and the plasticizer molecules.

3.3.2 | Relative permittivity

Figure 8 displays the EC content-dependence of the $\mathcal{E}$ in the MC: NaI system at 10^3 Hz. It is clear that $\boldsymbol{\varepsilon}$ and $\boldsymbol{\sigma}$ have the same trend and are both correlated to the concentration

TABLE 3 Relative permittivity values for polymer salt-complex with various amounts of ethyl carbonate (EC).

Samples	$\mathcal{E}$
MCSPE0	52.63
MCSPE1	850.33
MCSPE2	241.46
MCSPE3	760.83
MCSPE4	155.89

of carriers. The behavior of σ and $\mathcal{E}$ with the addition of EC can be impacted by two physical situations: 1) the blocking effect and 2) the space-charge-induced enhancing effect. The initial increase in ε is due to an increase in the number of charge carriers, followed by a further increase due to an increase in mobility.[45] In contrast, the second fall in ε found is driven by the blocking effect, which slows ion conduction due to increased charge concentrations that might no longer immobilize the polymer chain; this led to reduced segmental mobility and therefore decreased σ.[46] The initial increase in ε was due to the augmentation in carrier density and the subsequent decline was caused by the blocking layer effect which accumulates ion clusters in the plasticized SPE and limits the formation of ion-pair complexes. The intermediate increase of 30 wt. % EC is caused by the force of space charges that drives conducting ions and enhances σ. The final fall in dielectric constant was related to the accumulation of a high number of ion clusters that slowed down the polymer chain mobility which do not participate in the conductivity. The different values of ε were determined using Equations (2)–(4). Table 3 summarizes the values of ε for each content of EC in the plasticized SPE calculated at 10^3 Hz.

3.3.3 | Carriers density and mobility

Figure 9 displays the charge carrier density (n) and mobility (μ) with varying EC content in the SPE system at RT. It has been seen that carrier concentration and mobility are at odds with one another. After the addition of 10 wt. % EC, the initial increase in charge carriers followed by an increase of up to 40 wt. % EC is because of the increase of ion conductors in the polymer-salt complex which rises conductivity. The 20 wt. % drop is due to ion aggregations which do not impact on $\boldsymbol{\sigma}$. The presence of an overabundance of ion clusters in the SPE film causes a reduction in carrier density at high EC content. The limited density of charge carriers facilitates the movement of the polymer chain which improves its mobility. At elevated concentrations, salt in the MC+ 50 wt. % NaI matrix works as an ion supplier and as a plasticizing agent at lower concentrations, improving chain mobility. The density and mobility

Research Article
doi.org/10.1002/elsa.202300018
Chemistry Europe
European Chemical Societies Publishing

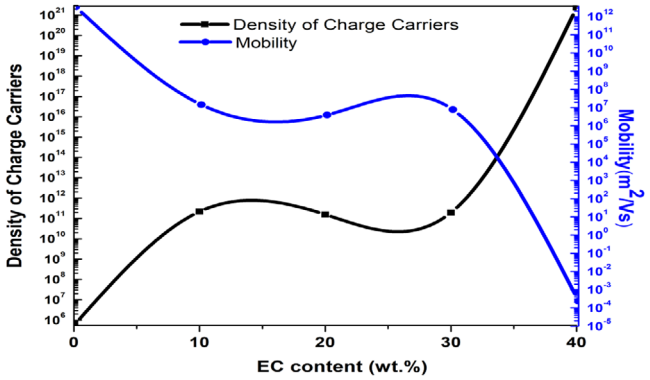

FIGURE 9 The variation of the carrier density and mobility with ethyl carbonate (EC) content in the MC+50 wt. % NaI system.

TABLE 4 The density of charge carriers and mobility values for various compositions of ethyl carbonate (EC) in the MC+50 wt. % NaI system.

EC content (wt. %)	Carriers density	Mobility (m^2/Vs)
0	5.50×10^5	3.43×10^{12}
10	2.19×10^{11}	14.44×10^6
20	1.58×10^{11}	3.95×10^6
30	1.97×10^{11}	7.77×10^6
40	2.39×10^{21}	2.37×10^{-4}

of charge carriers in plasticized SPE films are determined using Equations (5) and (6) and are shown in Table 4.

3.3.4 | Linear sweep voltammetry

The electrochemical stability window (ESW) for the optimized SPE film was obtained to be between +1.5 and -1 V. Figure 10 depicts the LSV data of the highly conductive sample: MC+50 wt. % NaI + 10 wt. % EC performed at scan rate of 100 mV/s throughout the potential range [−3, 3 V]. The electrochemical window value for the optimal plasticized SPE incorporated with EC was 2.5 V. The ESW was calculated using the prepared SPE embedded between two stainless steel plates (SS). The plasticized SPE's anodic voltammetry sweep revealed an oxidation onset at 1 V and a reduction onset at 1.5 V. It is evident that no anodic current is detected up to 0.975 V, proving that no chemical reactions occur within the plasticized SPE film in this range. The electrode potential rises over 1 V, and the current climbs steadily. This rise was caused by the deterioration of the electrolyte sample.[47] For protonic PEs and aqueous electrolytes, the typical potential window is approximately 1 V.[48] The obtained result indicates that the prepared SPE is thought to be suitable for energy storage device applications.

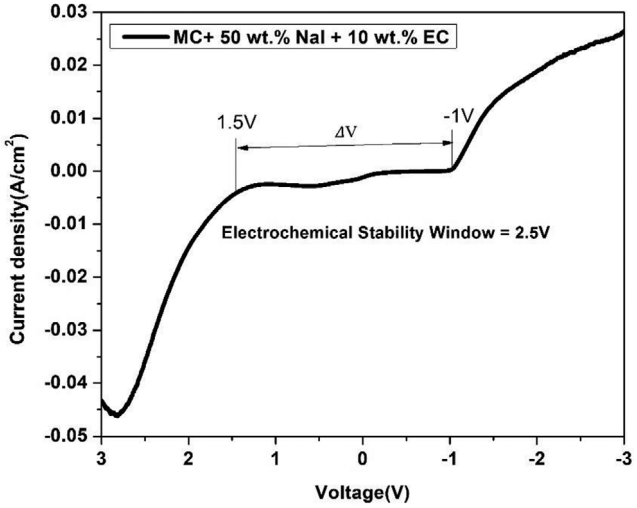

FIGURE 10 Linear sweep voltammetry (LSV) graph for the optimal plasticized solid polymer electrolyte (SPE) film recorded at scan rate 100 mV/s at room temperature (RT).

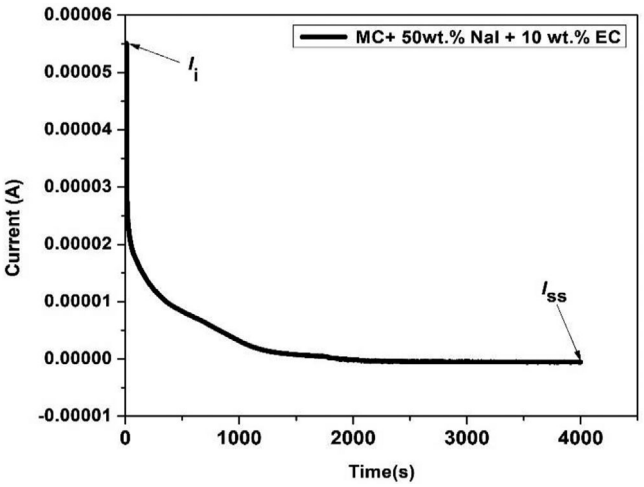

FIGURE 11 Time-dependent polarization current for the optimal plasticized solid polymer electrolyte (SPE) at an applied voltage of 0.8 V at room temperature (RT).

3.4 | Ionic transference number measurements

Ion and electron contributions to the overall conductivity of highly conductive PE were evaluated using Wagner's polarization. The cell: SS/ MC+ 50 wt.% NaI +10 wt.% EC /SS was polarized by applying a voltage of 0.8 V. A time-dependent vs. current density graph is depicted in Figure 11. The curve gradually declines until it achieves a steady-state current ($I_{ss} = 5.509 \times 10^{-7}$A). The total current ($I_i = 5.527 \times 10^{-5}$A) combines both ionic and electronic contributions at interface SS/SPE. I_{ss} confirms that the cell's polarization owing to the blocking effect of the SS electrodes, but it only allows electrons to flow through.[49–51]

Research Article
doi.org/10.1002/elsa.202300018
Chemistry Europe
European Chemical Societies Publishing

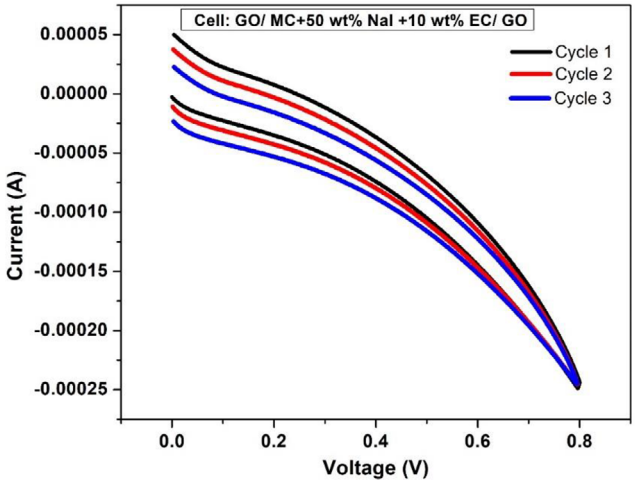

FIGURE 12 The optimized polymer electrolyte (PE) film-based supercapacitor's cyclic voltammetry (CV) plot was recorded at a scan rate of 50 mV/s over 0–0.8 V for the three first cycles.

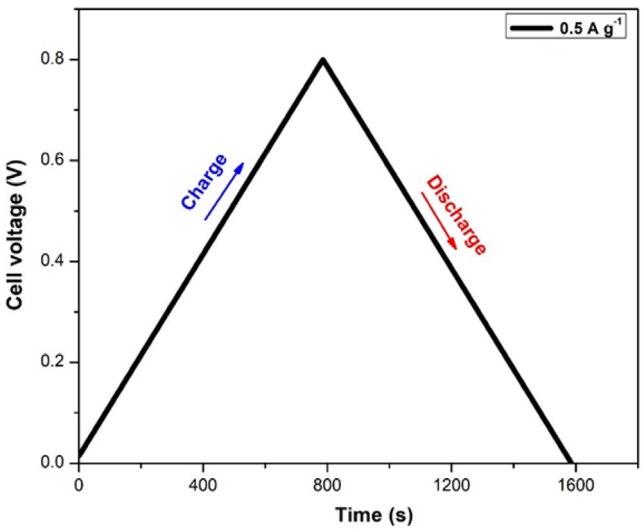

FIGURE 13 Galvanostatic charge-discharge (GCD) graph for electrical double-layer capacitor (EDLC) with the optimum solid polymer electrolyte (SPE) at room temperature at a constant current density of 0.5 A/g.

Ion contribution (t_{ion}) and electron contribution (t_{elec}) were computed using Equations (7) and (8) and determined to be 0.99 and 0.01, respectively. In PEs, sodium salts are dissolved in polymers to create cations and anions. The conductivity of NaI is due mainly to the migration of cation vacancies. Furthermore, much of the conductivity in PEs stems from the mobile anions, rather than the metal cations in energy storage. Because the contribution of electrons is so small, this result clearly shows that ions monitor conductivity. Plasticized SPE films are then found to be suitable for ionic devices.

3.5 | Cyclic voltammetry

The CV technique was used to test the supercapacitor's performance throughout a voltage range of 0–0.8 V. Figure 12 depicts the capacitive characteristics of the constructed supercapacitor, exhibiting the hysteresis buckle of a supercapacitor. The redox peak's absence, which denotes a non-faradaic mechanism during charge storage, confirmed the presence of the EDLC cell.[52] The anodic and cathodic peak potentials, as well as the corresponding anodic and cathodic peak currents, were not observed at 50 mV s^{-1} for the three first cycles. The CV graph shows that the total capacitance in the optimized sample ranges from 0 to 0.8 V, indicating the importance of surface area and narrow pore distribution.[53] The electrical field that separates the ion from the electrolyte and polarizes the electrons from the electrode charges the supercapacitor. The value of $C_{sp}$of the EDLC cell was computed from the CV curve using Equation (9) and determined to be 17.15 F g^{-1}.

3.6 | Galvanostatic charge-discharge

Figure 13 depicts the GCD graph of the manufactured GO-based supercapacitor. A constant current density of 0.5 A/g was applied to measure the potential versus time. The existence of internal resistance in the structure is shown by a voltage drop. The capacitor behavior of the design with a reduced Faradic process and low ESR value is shown by the linear charge/discharge curve, which indicates the supercapacitor is ideal. Equation (10) is used to calculate the coulombic efficiency of the GO-based system, and it is discovered to be 100%, indicating that the cell can sustain a load for a long time. Using Equation (11), the capacitive behavior of the supercapacitor was also estimated from the GCD curve illustrated in Figure 13. The estimated value of C_{sp} was 16.25 F/g at 0.5 A/g.

3.7 | Electrochemical impedance spectroscopy

The analysis of ionic transport, bulk electrolyte characteristics, behavior at the electrode-electrolyte interface, and other phenomena may be done effectively with EIS. This approach was used to study the impact of several variables on device performance, including charge-transfer resistance, electrolyte resistance, and C_{dl} at low frequencies. Figure 14 depicts the supercapacitor cell's low-frequency experimental impedance spectroscopy graph and fitting plot of the equivalent electrical circuit (EEC) across the frequency range 0.1 MHz to 5 mHz using the optimal SPE

Research Article
doi.org/10.1002/elsa.202300018
Chemistry Europe
European Chemical Societies Publishing

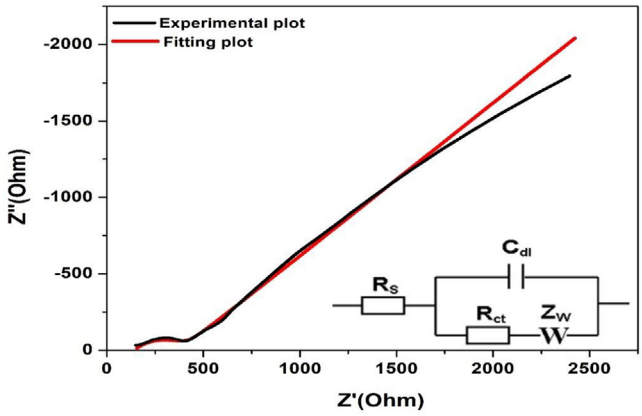

FIGURE 14 The fitting plot of experimental impedance and equivalent electrical circuit (EEC) for the optimized SPE: MC+50 wt%NaI+10 wt%.EC.

TABLE 5 Generated parameter values obtained with fitting data using the extrapolating graph approach in Origin Pro 8.0.[54]

Parameters/Unit	Value
R_s /Ω	90.51
R_{ct} /Ω	373
$C_{dl}/\mu F$	6.686×10^{-5}
$W/(\Omega/s^{1/2})$	16.47×10^{-4}
$-Z''/\Omega$	1715
C_{sp} /(F/g)	18.56

sample: MC+ 50 wt. % NaI + 10 wt.% EC. The modified Randal's equivalent circuit [54,55] which includes the electrolyte-electrode-current collector resistance (R_s), constant phase (Q) or double layer capacitance(C_{dl}), charge transfer resistance (R_{ct}) and Warburg component (W) as shown in Figure 14 was used to create the Nyquist plot. The bulk electrolyte and diffusion properties are essentially represented by R_{ct} and Z_w, but the dielectric and insulting properties at the electrode-electrolyte interface control QandR_{ct}. The capacitance between the electrolyte's ionic species and the electronic charges at the electrode surfaces is represented by C_{dl} in a parallel relationship with R_{ct}. The Nyquist plot assists in determining R_{ct}. The usual Nyquist plot has a semicircle component that represents the restricted phase of electron transfer at high frequencies and a linear portion that derives from the limited step of electrochemical diffusion at relatively low frequencies. The relative error of fitting was 0.5. The value of C_{sp} was calculated via Equation (12) and determined to be 18.56 F/g which is near to the obtained CV data. The values of the different parameters that were determined by fitting the impedance data with the EEC are shown in Table 5.

4 | DISCUSSION

According to a previous study [56] an unplasticized MC-based electrolyte (75 wt% MC-25 wt% NH_4NO_3) with a conductivity of 2.10×10^{-6} S/cm gives a low capacity of 1–2 F/g when utilized in a capacitor. In this investigation, because the plasticized sample (MC+ 50 wt. % NaI+10 wt.% EC) has a conductivity of 5.06×10^{-3} S/cm, the capacitance of the produced EDLC is expected to be higher (18.56 F/g). The CS: DN: NH4I: Zn (II) –the complex was plasticized with various GL concentrations, and the effects of the metal complex and GL on the electrolyte properties were investigated.[57] According to EIS studies, the plasticized system's greatest conductivity was 3.44×10^{-4} S/cm which was lower than that of our current study. TNM analysis revealed that the transport mechanism in the created electrolyte is primarily ionic, with a high value of $t_{ion} = 0.983$, which is less than 0.99 achieved with the optimized MC: NaI: EC system. LSV method revealed that the stability potential window of the CS: DN: NH4I: Zn electrolyte was 1.5 V. This value is found to be less than 2.5 V obtained with the LSV method for the optimized MC-based PE. Shujahadeen et al. developed an MC:Dextran (MC:Dex) based SPE doped with NH_4I for an EDLC application.[58] The highest conductivity was determined to be 1.12×10^{-3} S/cm for 40% NH_4I, which is lower than that of the optimal sample MC-NaI:EC system reported in this work using the same host polymer. The LSV investigation demonstrates that the ESW of the optimum sample: MC+50 wt. % NaI+10 wt. % EC (2.5 V) is greater than 1.27 V reported for the optimal MC:Dex:NH_4I electrolyte.

The current study, as well as prior studies, emphasizes the importance of biopolymers in PE synthesis and device manufacturing. In emerging technologies, the need for bendy energy storage devices such as EDLCs and batteries motivates experts to design and find novel materials. One challenge in this industry is that biopolymer-based devices are not strong for higher cycle numbers. Table 5 summarizes several essential parameters that can contribute to enhanced performance. To begin, choosing the host polymer matrix is a crucial element that plays a key role in achieving optimal results. In EDLC applications, the host polymer should have good electrochemical and thermomechanical properties. These features enable the manufactured EDLC device to provide good outputs and have a long cycle life. Second, when employing a PE in an electrochemical device, it is critical to choose an adequate dopant salt. Low lattice energy salts such as NaI facilitate dissociation, whereas high lattice energy salts are difficult to dissolve by the host polymer, which creates a lack of mobile carriers. Furthermore, the use of

Research Article
doi.org/10.1002/elsa.202300018
Chemistry Europe
European Chemical Societies Publishing

TABLE 6 A summary of the values of σ,t_{ion} and C_{sp} for previously developed electrolytes and the optimal sample MC+50 wt. % NaI+10 wt. % EC prepared in this work.

Samples	σ (S/cm) RT	t_{ion}(TNM)	$C_{sp}(F/g)$	References
[1]MC-NH_4NO_3	2.10×10^{-6}	–	1–2	[56]
[2]CS:DN:NH_4I:Zn(II)	3.44×10^{-4}	0.983	108.3	[57]
[3]MC:Dex:NH4I	1.12×10^{-3}	0.98	79	[58]
[4]CS:MC: NH_4SCN	2.81×10^{-3}	0.84	66.3	[59]
[5]MC-KI-glycerol	5.14×10^{-4}	0.964	68	[60]
[6]CS:MC:NH4I: glycerol	6.65×10^{-4}	0.97	9–10	[61]
[7]NaCMC/PVA-NaI	2.52×10^{-3}	0.99	–	[62]
[8]CS: NH_4NO_3:glycerol	3.21×10^{-3}	0.923	124	[63]
[9]MC-NaI	2.70×10^{-5}	–	–	[64]
[10]PVA-MC-NH_4I	7.01×10^{-8}	0.88	–	[65]
[11]MC–AF	6.40×10^{-7}	–	–	[66]
MC-NaI-EC	5.06×10^{-3}	0.99	18.56	Current work

[1]Methylcellulose(MC)-ammonium nitrate(NH_4NO_3).
[2]Chitosan (CS):dextran (DN):ammonium iodide (NH_4I):Zn(II)-metal.
[3]Methylcellulose (MC):Dextran(DN): ammonium iodide (NH_4I).
[4]Chitosan (CS): methylcellulose (MC):ammonium thiocyanate(NH4SCN).
[5]Methylcellulose (MC)- potassium iodide (KI)-glycerol.
[6]Chitosan (CS):methylcellulose (MC): ammonium iodide (NH_4I): glycerol.
[7]Sodium carboxymethyl cellulose (NaCMC)/poly(vinyl alcohol) (PVA)-sodium iodide (NaI).
[8]Chitosan (CS):ammonium nitrate(NH_4NO_3):glycerol.
[9]Methylcellulose(MC)-Sodium Iodide(NaI).
[10]Polyvinyl alcohol(PVA)-methylcellulose (MC)- ammonium iodide (NH4I).
[11]Methylcellulose (MC)- ammonium fluoride(AF).

plasticizers such as EC can facilitate ionic conduction; nevertheless, a substantial quantity can generate mechanical weakness and rise reactivity about electrodes. Our research group is working to create PE sheets that have high device performance and conductivity. As far as we know, all biopolymer-based outcomes should be disclosed in other to highlight the advancements made in this sector. The outcomes indicate the potential for future high-performance gadget development; nevertheless, further attention from scientists is required. Biopolymer-based devices must be prioritized since they are completely non-toxic and do not include any harmful components. As previously stated, several parameters such as functional groups of the polymer, salt lattice energy, and plasticizers have an impact on device performance. As a consequence, these parameters should be investigated early and findings should be also reported. However, the performance of EDLC devices based on biopolymers has been encouraging thus far, and improved performance is predicted shortly. Table 6 displays the σ, $t_{ion}$and C_{sp} measurements made for the latest developed solid bioPEs and the currently used PEs. According to the findings, this study improves electrolyte characteristics and device performance above some earlier results.

5 | CONCLUSIONS

New plasticized SPEs based on biopolymer (MC), NaI salt as a dopant, and EC as a plasticizing agent have been successfully developed using the solution cast technique. The plasticized electrolyte samples exhibited outstanding properties which were suitable for supercapacitor devices. The inclusion of EC in the MC: NaI matrix has improved the electrochemical and physical properties of the plasticized SPEs and the optimal sample containing EC was tested in a solid-state EDLC to evaluate its performance. The highest conductivity of the optimal plasticized SPE film was 5.06×10^{-3} S/cm for the composition: MC+50 wt. % NaI+10 wt. % EC and was electrochemically stable up to 2.5 V. The plasticized PE with the highest conductivity is amorphous and flexible. At relatively low EC concentrations, the film is also characterized by smoothness and homogeneity of surface shape. The dominance of ions over electron conductions within the electrolyte was confirmed as expected with 99% of ion contribution to conductivity. The developed gel polymer films were free-standing and flexible with good electrochemical and mechanical properties which are suitable for solid-state supercapacitors. GCD data shows that the Columbic efficiency of the

Research Article
doi.org/10.1002/elsa.202300018
Chemistry Europe
European Chemical Societies Publishing

EDLC device based on the prepared optimal film was 100% and its specific capacitance was 18.56 F/g. According to the findings presented in this paper, these newly created electrolytes are desired options among other electrolytes for not only flexible solid-state supercapacitors but also the fabrication of innovative batteries with higher safety, flexibility, and cycling stability.

AUTHOR CONTRIBUTIONS

Conceptualization, Theodore Manfo Azemtsop; methodology, Theodore Manfo Azemtsop ; software, Theodore Manfo Azemtsop; validation, Theodore Manfo Azemtsop, formal analysis, investigation, Theodore Manfo Azemtsop; resources, Theodore Manfo Azemtsop; data curation, Theodore Manfo Azemtsop; writing—original draft preparation, Theodore Manfo Azemtsop; writing—review and editing, Theodore Manfo Azemtsop; visualization, Theodore Manfo Azemtsop; supervision, Theodore Manfo Azemtsop; project administration, Theodore Manfo Azemtsop; funding acquisition, Theodore Manfo Azemtsop. The authors have read and agreed to the published version of the manuscript.

ACKNOWLEDGMENTS

The author wishes to thank the staff of the Department of Physics, Sharda University (India), Prof. Mustafa Ergin SAHIN from the Department of Electric and Electronic Engineering, RTEU (Turkey) for the contributions.

CONFLICT OF INTEREST STATEMENT

The author declares no conflict of interest.

FUNDING INFORMATION

The author has not received any funds for this work.

DATA AVAILABILITY STATEMENT

The author's data for this work is freely available upon request.

ORCID

Theodore Manfo Azemtsop https://orcid.org/0000-0002-9043-3111

REFERENCES

1. K. D. Fong, T. Wang, S. K. Smoukov, *Sustain. Energy Fuels J.* **2017**, *1*, 1857.
2. M. Ates, *J Solid State Electrochem.* **2016**, *20*, 1509.
3. D. Pech, M. Brunet, H. Durou, P. Huang, V. Mochalin, Y. Gogotsi, P.-L. Taberna, P. Simon, *Nat. Nanotechnology.* **2010**, *5*, 651.
4. S. K. Patla, A. R. Choudhury, R. Ruma, S. Das, S. Karmakar, *AIP Adv.* **2020**, *10*, 115008.
5. A. N. A. Nik, N. K. Idris, M. I. N. Isa, *Int. J. Polym. Anal. Charact.* **2010**, *15*, 319.
6. R. Mantravadi, P. R. Chinnam, D. A. Dikin, S. L. Wunder, *ACS Appl. Mater. Interfaces.* **2016**, *8*, 13426.
7. M. N. Chai, M. I. N. Isa, *J. Cryst. process technol.* **2013**, *3*, 1.
8. F. M. Gray (Ed.), *Solid Polymer Electrolytes: Fundamentals and Technological Applications*, VCH Publishers Inc., New York**1991**.
9. M. T. Taghizadeh, P. Seifi-Aghjekohal, *Ultrason. Sonochem.* **2015**, *26*, 265.
10. A. F. M. Shukur, Ph.D. Thesis, University of Malaya, Kuala Lumpur, Malaysia **2015**.
11. S. B. Aziz, I. Brevik, M. H. Hamsan, M. A. Brza, M. M. Nofal, A. M. Abdullah, S. Rostam, S. Al-Zangana, S. K. Muzakir, M. F. Z. Kadir, *Polymers.* **2020**, *12*, 2257.
12. M. A. Brza, S. B. Aziz, H. Anuar, F. Ali, M. H. Hamsan, M. F. Z. Kadir, R. T. Abdulwahid, *Arab. J. Chem.* **2020**, *13*, 7247.
13. a) S. A. Alexandre, G. G. Silva, R. Santamaría, P. C. João, J. P. C. Trigueiro, R. L. Lavall, *Electrochim. Acta.* **2010**, *299*, 789. b) S. B. Aziz, Z. H. Z Abidin, A. K. Arof, *J. Phys. B: At. Mol. Opt. Phys.* **2010**, *405*, 4429.
14. M. H. Hamsan, M. F. Shukur, M. F. Z. Kadir, *Ionics.* **2017**, *23*, 3429.
15. S. B. Aziz, M. H. Hamsan, R. M. Abdullah, M. F. Z. Kadir, *J. Mater. sci. technol.* **2019**, *24*, 2503.
16. S. B. Aziz, M. A. Brza, K. Mishra, M. H. Hamsan, W. O. Karim, R. M. Abdullah, M. F. Z. Kadir, R. T. Abdulwahid, *J. Mater. Res. Technol.* **2020**, *9*, 1137.
17. C. V. S. Reddy, A.-P. Jin, Q. Y. Zhu, L.-Q. Mai, W. Chen, *EPJ E* **2006**, *19*, 471.
18. A. M. Abdullah, S. B. Aziz, S. R. Saeed, *Arab. J. Chem.* **2021**, *14*, 103388.
19. C. V. Ismayil, I. M. Noor, K. Mishra, C. Chavan, R. F. Bhajantri, S. P. Masti Ionic, *Cellul.* **2020**, *29*, 3271.
20. S. B. Aziz, Z. H. Z. Abidin, *J. Appl. Polym. Sci.* **2015**, *132*, n/a.
21. H. J. Schutt, E. Gerdes, *J Non-Cryst Solids.* **1992**, *144*, 14.
22. R. T. Abdulwahid, S. B. Aziz, M. A. Brza, M. F. Z. Kadir, W. O. Karim, H. M. Hamsan, S. F. Ahmad, M. Asnawi, R. M. Abdullah, M. M. Nofal, E. M. A. Dannoun, *J Mater Sci Mater Electron.* **2021**, *32*, 14846.
23. S. Konwar, P. S. Dhapola, M. Gupta, R. C. Singh, *Macromolecular Symposia.* **2019**, *388*, 1900038.
24. G. P. Pandey, Y. Kumar, S. A. Hashmi, *Solid State Ion.* **2011**, *190*, 93.
25. S. B. Aziz, M. G. Faraj, O. G. Abdullah, *Sci. Rep.* **2018**, *8*, 14308.
26. X. Huang, T. Ren, L. Tian, L. W. Z Hong, X. Tang, *J. Mater. Sci.* **2004**, *39*, 1221.
27. S. B. Aziz, R. M. Abdullah, *Electrochim. Acta.* **2018**, *285*, 30.
28. G. Jo, H. Ahn, M. J. Park, *ACS Macro Lett.* **2013**, *2*, 990.
29. M. F. Shukur, R. Ithnin, M. F. Z. Kadir, *Ionics.* **2014**, *20*, 977.
30. S. B. Aziz, S. Al-Zangana, H. J. Woo, M. F. Z. Kdir, O. G. Abdullah, *Results in Phys.* **2018**, *11*, 826.
31. M. H. Buraidah, A. K. Arof, *J Non-Cryst Solids.* **2011**, *357*, 3261.
32. M. N. Chai, M. I. N. Isa, *Int. J. Polym. Anal.* **2013**, *18*, 280.
33. S. N. Bhad, V. S. Sangawar, *Int. j. sci. eng. res.* **2013**, *4*, 1719.
34. M. A. Saadiah, Y. Nagao, A. S. Samsudin, *Int. J. Hydrog. Energy.* **2021**, *46*, 17231.
35. L. Fan, Z. Dang, C. W. Nan, M. Li, *Electrochim. Acta.* **2002**, *48*, 205.
36. P. B. Bhargav, V. M. Mohan, A. K. Sharma, V. V. R. N. Rao, *Ionics.* **2007**, *13*, 441.

Research Article
doi.org/10.1002/elsa.202300018
Chemistry Europe
European Chemical Societies Publishing

37. A. N. A. Nik, N. K. Idris, M. I. N. Isa, *Int. J. Polym. Anal.* **2010**, *15*, 319.
38. A. S. Samsudin, W. M. Khairul, M. I. N. Isa, *J Non Cryst Solids.* **2012**, *358*, 1104.
39. N. S. Salleh, S. B. Aziz, Z. Aspanut, M. F. Z. Kadir, *Ionics.* **2016**, *22*, 2157.
40. S. Iqbal, H. Khatoon, A. H. Pandit, S. Ahmad, *Mater. Sci. Technol.* **2019**, *2*, 417.
41. L. Bach-Toledo, B. M. Hryniewicz, L. F. Marchesi, H. Luiz, L. H. Dall'Antonia, M. Vidotti, F. Wolfart, *Mater. Sci. Technol.* **2020**, *3*, 78.
42. P. H. Maheshwari, *Mater. Sci. Technol.* **2019**, *2*, 490.
43. P. M. Anjana, M. R. Bindhu, R. B. Rakhi, *Mater. Sci. Technol.* **2019**, *2*, 389.
44. S. R. Eedulakanti, A. K. Gampala, K. V. Rao, C. S. Chakra, G. Venkataramana, B. Rajender, *Mater. Sci. Technol.* **2019**, *2*, 372.
45. A. T. Manfo, S. Konwar, P. K. Singh, R. M. Mehra, Y. Kumar, M. Gupta, *Proc. Mater.* **2021**, *34*, 802.
46. A. T. Manfo, P. K. Singh, R. M. Mehra, R. C. Singh, M. Gupta, *Recent Innov. Chem. Eng.* **2021**, *14*, 21.
47. L. Sampathkumar, P. C. Selvin, S. Selvasekarapandian, P. Perumal, R. Chitra, M. Muthukrishnan, *Ionics.* **2019**, *25*, 1067.
48. R. Pratap, B. Singh, S. Chandra, *J. Power Sources.* **2006**, *161*, 702.
49. C. Devi, J. Gellanki, H. Pettersson, S. Kumar, *Sci. Rep.* **2021**, *11*, 20180.
50. M. S. A. Rani, A. Ahmad, N. S. Mohamed, *Ionics.* **2018**, *24*, 807.
51. M. Z. Kufian, M. F. Aziz, M. F. Shukur, A. S. Rahim, N. E. Ariffin, *Solid State Ion.* **2012**, *208*, 36.
52. G. P. Pandey, Y. Kumar, S. A. Hashmi, *Solid state Ion.* **2011**, *190*, 93.
53. N. Badi, A. M. Theodore, S. A. Alghamdi, H. A. Al-Aoh, A. Lakhouit, A. S. Roy, A. S. Alatawi, A. Ignatiev, *Polymers.* **2022**, *14*, 3837.
54. G. H. Xu, C. Zheng, Q. Zhang, J. Huang, M. Zhao, J. Nie, X. Wang, W. Fei, *Nano Res.* **2011**, *4*, 870.
55. A. D. Fabio, A. Giorgi, M. Mastragostino, F. Soavi1, *J. Electrochem. Soc.* **2001**, *148*, A845.
56. N. E. A. Shuhaimi, S. R. Majid, A. K. Arof, *Mater. Res. Innov.* **2009**, *13*, 239.
57. M. H. Hamsanm, M. M. Nofal, S. B. Aziz, M. A. Brza, M. A. E. Dannoun, A. R. Murad, M. F. Z. Kadir, S. K. Muzakir, *Polymers* **2021**, *13*, 1233.
58. S. B. Aziz, M. A. Brza, K. Mishra, M. H. Hamsan, W. O. Karim, R. M. Abdullah, M. F. Z. Kadir, R. T. Abdulwahid, *Mater. Sci. Technol.* **2020**, *9*, 1137.
59. S. B. Aziz, M. H. Hamsan, R. M. Abdullah, M. F. Z. Kadir, *Molecules.* **2019**, *24*, 2503.
60. S. B. Aziz, E. M. A. Dannoun, R. T. Abdulwahid, M. F. Z. Kadir, M. M. Nofal, S. I. Al-Saeedi, A. R. Murad, *Membranes* **2022**, *12*, 139.
61. S. B. Aziz, M. H. Hamsan, M. A. Brza, M. F. Z. Kadir f, S. K. Muzakir, R. T. Abdulwahid, *J. Mater. Res. Technol.* **2020**, *9*, 8355.
62. C. V. Ismayil, I. M. Noor, K. Mishra, C. Chavan, R. F. Bhajantri, S. P. Masti, *Cellul.* **2022**, *29*, 3271.
63. S. B. Aziz, M. A. Brza, I. Brevik, M. H. Hamsan, R. T. Abdulwahid, S. R. Majid, M. F. Z. Kadir, S. A. Hussen, R. M. Abdullah, *Polymers.* **2020**, *12*, 2718.
64. J. F. Z Abiddin, A. H. Ahmad, *J. Teknol.* **2015**, *76*, 41.
65. M. M. Nofal, S. B. Aziz, M. A. Brza, S. N. Abdullah, E. M. A. Dannoun, J. M. Hadi, A. R. Murad, S. I. Al-Saeedi, M. F. Z. Kadir, *Membr.* **2022**, *12*, 284.
66. N. A. N. Aziz, N. K. Idris, M. I. N. Isa, *IJPS.* **2010**, *5*, 748.

How to cite this article: T. M. Azemtsop, *Electrochem Sci Adv*. **2023**, e2300018.
https://doi.org/10.1002/elsa.202300018

AUTHOR BIOGRAPHY

Dr. Theodore Azemtsop Manfo received the B.S. and M.S. degrees in physics from the University of Yaounde I, in 2015 and the Ph.D. degree in Physics from Sharda University, Greater Noida, Uttar Pradesh, India, in 2021. Since 2016, he has been a lecturer at the Department of Physics, Laboratory of Material Science at the University of Yaounde I. He was a Postdoctoral Researcher at Sharda University in India 2021–2022. He is now Visiting Researcher at Recep Tayyip Erdogan University, Turkey in the Department of Electrical and Electronic Engineering. He is working on supercapacitors, batteries, and conversion systems for industrial applications.